Particle Accelerators
1980, Vol. 11, pp. 45-62
0031-2460/80/1101-0045 $06.50/0

HIGH-MODULATION ELECTRON BEAMS IN STORAGE RINGS

PAUL L. CSONKA

Institute of Theoretical Science, University of Oregon, Eugene, Oregon 97403 U.S.A.

(Received June 15, 1979; in final form August 13, 1979)

Electron beams whose density ρ changes (is modulated) rapidly as a function of position z along the orbit are generally desirable for coherence and correlation experiments. When $\rho(z)$ changes significantly within an optical wavelength or less, and if the number of electrons within a z interval of this wavelength is $n \gg 1$, the radiation emitted will differ importantly from radiation emitted by more usual beams: the angular spread will decrease (brightness will increase), the total intensity will increase by a factor of approximately n (including the x-ray region), certain wavelengths may be suppressed, and high time-resolution measurements are facilitated. Applications suggest themselves to holography, x-ray lasers, free electron lasers, etc. A method is described whereby high beam-density modulation can be induced in a storage ring with an optical laser of modest power, and the energy spread of the circulating beam is further reduced by compensation.

I. INTRODUCTION

Electromagnetic radiation from electron storage rings is usually produced in short bursts lasting about 10^{-9} to 10^{-10} seconds. This rapid time variation of the emitted radiation proves to be of great value. Exploiting it, one can increase the signal-to-noise ratio, improve the accuracy of decay time measurements, and so forth.

The value of rapid intensity variation can be traced to the fact that the intensity as a function of time $I(t)$ is rich in Fourier components. Indeed, if the radiation is emitted in bursts which last a time τ, $I(t)$ has Fourier components $F(\omega)$ with appreciable amplitude up to circular frequencies $\omega \approx 2\pi\tau^{-1}$, up to about 10^{10} to 10^{11} sec^{-1} for most electron storage rings. The presence of rapidly time-varying Fourier components in $I(t)$ is in turn caused by the richness in Fourier components of the circulating electron density, ρ, as a function of z, where z measures the position along the trajectory: The radiation intensity depends on the density of electrons passing before the port at the moment of emission. Since all electrons travel with velocity $v \approx c$, presence of a Fourier component in ρ, which varies as $\exp[i2\pi z/\lambda_m]$, will cause the appearance of a Fourier component in $I(t)$, with $\omega \approx 2\pi c/\lambda_m$. We refer to λ_m as the electron-density "modulation wavelength". For most storage rings $\rho(z)$ contains Fourier components with appreciable amplitude for $\lambda_m \gtrsim 3$ cm–30 cm.

Not surprisingly, whole new classes of experiments would become feasible if one could further enrich $I(t)$ in Fourier components, i.e., if a $\rho(z)$ could be produced which contains significant amounts of Fourier components with λ_m even lower than usual. The improvement in storage-ring capability would become truly spectacular about when the modulation is so high that $\lambda_m \lesssim 10^{-4}$ cm (for high enough ρ).

The fact that richness of Fourier components leads to a richness of experimental results has been well understood after the Heisenberg uncertainty principle became known. It led to the construction of higher and higher energy particle beams to reach higher frequencies and shorter wavelengths. But these beams are usually used in experiments where correlations between particles in the same beam are of little importance. The experimental result can be obtained by simply summing over the result produced by each beam particle alone. On the other hand, in more complex experiments the correlation between beam particles becomes important, and can generate experimental consequences that are not reproducible by adding the results which would be obtained by each beam particle acting alone. Broadly speaking, the phenomena generated by correlations become richer when the correlations between beam particles are richer in Fourier components, analogously to how higher momentum and energy enrich the observable single-particle phenomena. In this sense, high-modulation beams have the same importance in many-particle (correlation, coherence) experiments, as high-energy beams do in single-particle experiments.

Next we briefly survey certain characteristics of high-modulation beams, and recall some of their possible applications. Finally we describe a method whereby such beams can be produced using a laser of moderate power.

II. CHARACTERISTICS OF HIGH-MODULATION BEAMS

The density of ideal circulating electrons as a function of z (the position along the design orbit) can be written as a sum of Fourier components

$$\rho(z) = \sum_{\lambda_m=\lambda_M}^{L_0} a_m e^{i2\pi z/\lambda_m}, \qquad (1)$$

where L_0 is the circumference of the design orbit, and $a_m = a^*_{-m}$, because $\rho(z)$ is real.

1. Rapidly Varying $I(t)$

As noted earlier, for a high-modulation beam the photon intensity $I(t)$ as a function of time will have high-frequency Fourier components. When $\lambda_m \lesssim 10^{-4}$ cm, $\omega \gtrsim 1.9 \cdot 10^{15}$ sec^{-1}.

2. High Radiated Intensity

To simplify discussion, we will assume for the moment that $\rho(z)$ contains only one Fourier component with wavelength λ_m, i.e., $a_{m'} = \delta_{m',m}$. (The more general case is a straightforward extension of this simple one.) We also assume that the number n of electrons located within a z interval of length λ_m is

$$n = \int_0^{\lambda_m} \rho(z)\, dz \gg 1. \qquad (2)$$

For densities high enough to satisfy condition (2), the intensity of the electromagnetic radiation emitted by a high-modulation beam can be much higher than for a usual beam (i.e., one with more slowly varying density distribution). More precisely, it can be shown that[1,2] for a radiation wavelength $\lambda \approx \lambda_m$, the radiated intensity may be of the order of n times higher than for usual beams. In particular, we shall see that using an optical laser, one can set up a high-modulation electron beam in which λ_m is of the order 10^{-3} to 10^{-6} cm or even shorter, and which can, therefore, radiate orders of magnitude more photons in the microwave, optical and x-ray regions than usual beams would.

3. High Brightness. Compressed Radiated Angular Distribution.

Assume that $\rho(z)$ contains several Fourier components that combine to produce a density distribution shown by the solid line in Fig. 1. To simplify discussion, we idealize this type of density distribution by a step function-like distribution, shown by the dashed line. For the idealized distribution, the electron beam would have a bunch structure as shown in Fig. 2. The rectangular slabs shown in the figure are uniformly filled with electrons; the space between slabs is empty.

In the instantaneous rest frame of the beam, the slabs are at rest, although the electrons inside them oscillate and thus emit radiation. The radiation may consist of several Fourier components. Let us concentrate our attention on one of these, that which has wavelength $(\lambda)'$. (The prime outside the parentheses means that the quantity is measured in the instantaneous restframe of the beam.) If the thickness of each slab, $(\Delta z)'$, satisfies $(\Delta z)' \lesssim (\lambda)'/8$, then for radiation of wavelength $(\lambda)'$ impinging on it, each slab will radiate essentially as a plane mirror of width $(\Delta x)'$ and height $(\Delta y)'$, i.e., as a rectangular slit with these same dimensions.[2] Most of the radiation will be contained within the first interference maximum; its horizontal and vertical angular-half widths near the forward direction are

$$\tfrac{1}{2}(\Delta\theta_x)' = \frac{(\lambda)'}{(\Delta x)'}$$
$$\tfrac{1}{2}(\Delta\theta y)' = \frac{(\lambda)'}{(\Delta y)'}. \qquad (3)$$

Actually, Eqs. (3) hold only if the electron density within each slab is uniformly smeared out. Real electron distributions are not like that, but Eqs. (3) are still approximately valid, provided that the electron distribution is approximately uniform and that there is at least one electron for each $[(\lambda_m)'/4]^2$ area of the (x,y) surface of each slab, i.e., provided that the number of electrons in a slab-shaped bunch satisfies

$$N \gtrsim (\Delta x)' \cdot (\Delta y)'/(\lambda_m^2)'. \qquad (4)$$

Viewed from the laboratory frame, the angles are Lorentz contracted, so that (unprimed quantities refer to the laboratory frame) with $\gamma = (1 - v^2/c^2)^{1/2}$,

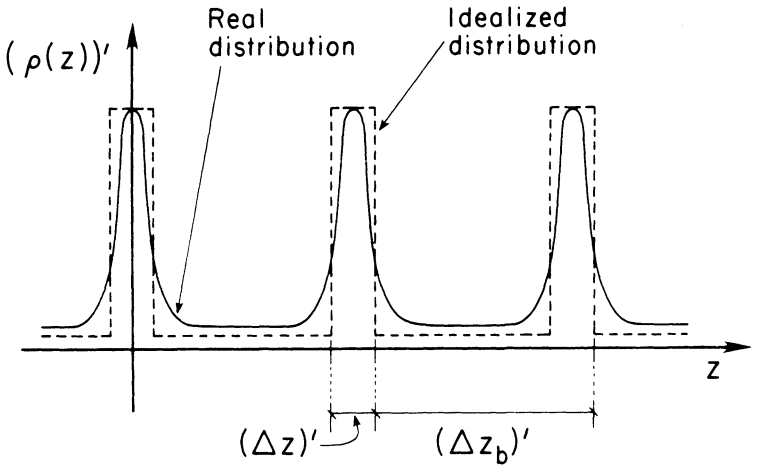

FIGURE 1. The electron density ρ as a function of z (the position along the design orbit) is shown by the solid line. This distribution is approximated by the step-function-like (unrealistic) distribution curve illustrated by the dashed curve. A prime on a quantity in brackets [e.g., $(z)'$] means that the quantity is measured in the beam rest frame.

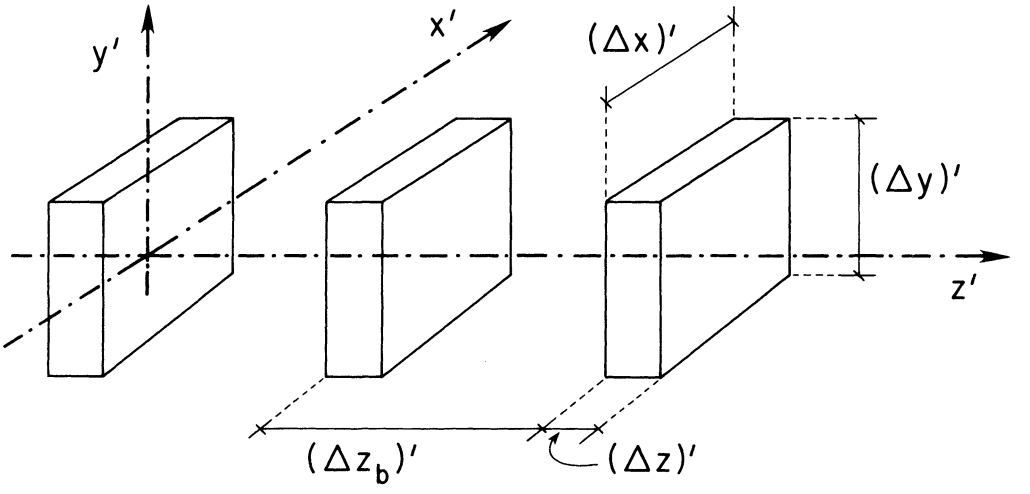

FIGURE 2. The electron density $(\rho)'$ is assumed to have a step-function-like dependence on $(z)'$ (as shown by the dashed line in Fig. 1) and also on $(x)'$ and $(y)'$. Viewed from the rest frame of the electron beam, such an idealized electron beam consists of a series of slabs, each uniformly filled up with electrons, and with no electrons between the slabs. Quantities measured in the beam restframe are denoted as in Fig. 1.

$$\begin{aligned} \tfrac{1}{2}\Delta\theta_x &= \frac{\lambda}{\Delta x} \approx \tfrac{1}{2}\frac{(\lambda)'}{\Delta x}\frac{1}{\gamma}, \\ \tfrac{1}{2}\Delta\theta_y &= \frac{\lambda}{\Delta y} \approx \tfrac{1}{2}\frac{(\lambda)'}{\Delta y}\frac{1}{\gamma}. \end{aligned} \qquad (5)$$

In Eqs. (5), we have used the fact that for photons emitted near the forward direction in the beam rest frame $\lambda \approx (\lambda)'/2\gamma$.

Single electrons (or several incoherently acting electrons) emit synchrotron radiation within the

typical angle $\frac{1}{2}\Delta\theta_0 \approx \gamma^{-1}$. Equations (5) show that as a result of the assumed beam structure, the emitted electromagnetic radiation (including synchrotron radiation) is confined to angles of order $\lambda/\Delta x$ and $\lambda/\Delta y$ times less in the horizontal and vertical planes, respectively. Thus the brightness of the emitted radiation will increase[3] by a factor of $\Delta y/\lambda$, or $\Delta x \cdot \Delta y/\lambda^2$, even if the total radiation intensity is unchanged. For example, when $\Delta x \cdot \Delta y > 10^2\,\lambda$, in principle[3] one can increase brightness by a factor 10^4 even without and beyond that which results from the increase of total intensity described in the previous section.

Furthermore, for this reason, one can increase the cross section of a high-modulation beam (and perhaps put more electrons in a bunch) without a proportional deterioration of photon focusability.

4. *Modifying the Energy Spectrum*

The idealized beam structure depicted in Fig. 2 resembles a crystal in that here too, the radiating electrons are confined to regularly spaced parallel surfaces. Consider again that Fourier component of the radiation which has wavelength $(\lambda)'$ and is emitted at an angle $(\theta_x)', (\theta_y)'$ (measured in the beam restframe). If $(\Delta z)' \ll (\lambda)'$, then each electron bunch of length $(\Delta z)'$, can be considered to be approximately a single plane. One can then use the Bragg conditions to calculate which frequencies will be suppressed and which will be enhanced for any given θ_x and θ_y. Since the planes are far from infinite in extension along x and y, higher interference orders have to be considered. The phenomenon becomes particularly simple[4] when $(\Delta x)', (\Delta y)' \ll (\lambda)'$.

Experiments where the above characteristics would be important include the following:

High-accuracy (decay) time measurements, by means of phase-shift observation on a Fourier component of $I(t)$. A.P. Sabersky and I.H. Munro[5] were the first to perform such measurements on a storage ring. An experiment is now in progress[6] at SPEAR where the Fourier component used is the thirty-fifth harmonic of the revolution frequency to achieve 3-psec time resolution. In this kind of experiment, the accuracy generally increases as the frequency of the used Fourier component increases. For high-modulation beams, one could have $\omega \gtrsim 2 \cdot 10^{15}\ \text{sec}^{-1}$.

X-ray holography. Pumping x-ray lasers with synchrotron radiation.

Both of the above require high instantaneous brightness, which could be provided by high-modulation beams.

X-ray lasers can themselves be utilized to "bootstrap" the beam modulation wavelength to lower values. This will be explained below.

Free-electron lasers. When high-modulation beams are sent into the laser, the lasing threshold can be lowered, and the power output increased. The energy separator described in the next section makes it possible to raise the power output beyond what is considered at present to be its theoretical upper limit.[7] The method of compensation also described, further improves performance.

In all such experiments it is the high modulation of the beam which yields the high radiation intensity, whatever may be the nature of forces which accelerate the electron bunches at the moment of photon emission. Those forces can be magneto static (as in a bending magnet or static wiggler) electromagnetic (e.g. a travelling wave in an undulator or free electron laser), etc.

The desirable features of high modulation beams (intensity, brightness, spectrum, time structure) and the variety of experiments which could utilize them suggest that in future storage rings intended wholly or partly for photon generation, the option to produce high modulation beams should be available. The devices (to be described below) which can produce such beams should be kept in mind in the design work, and, at the least, space should be provided where they can be installed.

III. PRODUCTION OF HIGH-MODULATION BEAMS

We describe a method in which high beam modulation is achieved in four steps.[8]

First, the angular spread of the beam is decreased. Second, a strong correlation is induced between the circulating electron energy and one of the transverse coordinates (say x) by a device referred to as the "energy separator." Third, the electron energies are altered by the "energy modulator"; and finally, fourth, beam-density modulation is produced in the "beam buncher."

We begin by describing the last two steps, and then return to the first two.

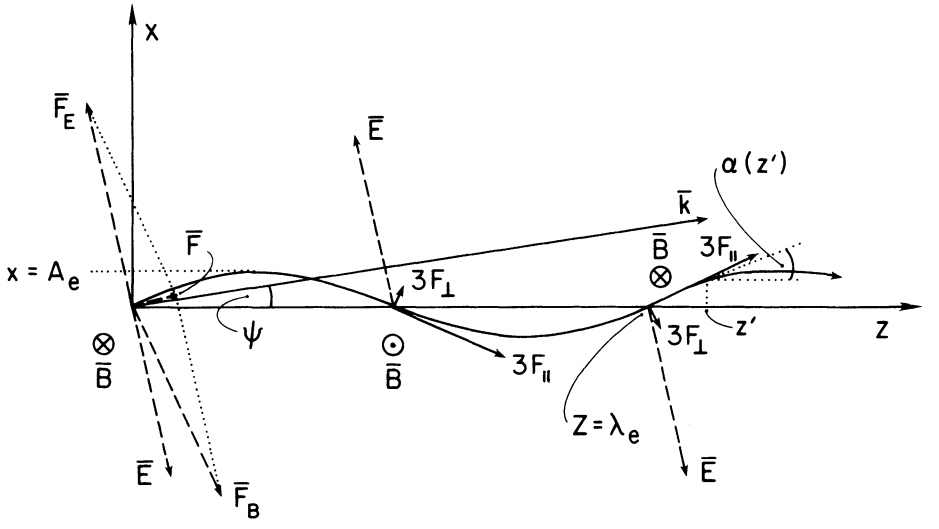

FIGURE 3. In the energy modulator, the electrons travel along a path resembling a sine wave (solid line). The curve is periodic with a wavelength λ_e, its amplitude is A_e. The slope of the path at z is $tg\,\alpha(z)$, $\alpha(z)$, α is shown for one particular $z = z'$ value. A plane electromagnetic wave of wavelength λ travels parallel to the $[x,z]$ plane (λ can be $\ll \lambda_e$ and is not shown). The momentum $\mathbf{k}$ of the wave makes an angle ψ with the z axis. The electric and magnetic fields associated with the wave, $\mathbf{E}$ and $\mathbf{B}$ respectively, are illustrated for three z values. The electric and magnetic force exerted on an electron at some point z by the wave, $\mathbf{F}_E(z)$ and $\mathbf{F}_B(z)$ respectively, is shown at one point. The total electromagnetic force $\mathbf{F} = \mathbf{F}_E + \mathbf{F}_B$ has component $F_\parallel$ and $F_\perp$ parallel and perpendicular to the electron path. For better visibility, $3F_\parallel$ and $3F_\perp$ (rather than $F_\parallel$ and $F_\perp$) are shown for three values of z.

In certain cases some of the following four additional steps may also be desirable: refocusing, defocusing, beam debunching, beam demodulation. These four steps will be discussed last.

Energy Modulator. Assume for the time being that all electrons move along the design orbit, i.e., their energy and momentum spreads are zero. We will later consider the effect of finite ΔE and $\Delta\bar{p}$.

In the energy modulator, the electrons move along a sinusoidal path. During their motion they interact with a plane electromagnetic wave. The mechanism that modulates the electron energy is essentially that which is employed for microwave generation in undulators[9] (see Fig. 3). Note that in the device to be described here, the axis of the curve along which the electrons move (the z axis) may not be parallel to the line along which the electromagnetic wave propagates.

Let the electrons move along a curve which resembles a sine wave of wavelength λ_e and amplitude A_e (see Fig. 3). The amplitude A_e depends on the electron energy E_e, while λ_e is independent of E_e to a very good approximation. In practice it is easier to achieve electron paths that are not sinusoidal, but for which every period of the curve is formed by a sequence of two smoothly joined circular arcs. The deviation of such a path from a true sine curve will be of the order $(A_e/\lambda_e)^3$, small when $A_e \ll \lambda_e$. Curves consisting of a sequence of circular arcs can be realized by letting the electrons traverse a section-wise-constant magnetic field in which the field has equal magnitude in all sections but switches sign at each boundary between sections. In the following we assume that the electrons follow a sinusoidal path to an adequate approximation.

The electron path lies in the (x,z) plane; the z axis is parallel to the axis of the sine curve. The x and z coordinates of the electron are given at any time t by

$$x(t) = A_e \sin \frac{2\pi}{\lambda_e} z(t), \tag{6a}$$

$$z(t) = z_0 + v_z (t - t_0) \tag{6b}$$

Let v_x and v_z be the x and z components of the electron velocity $\mathbf{v}_e$, and $\tilde{v}_z$ the average (over t) of v_z. The electron velocity makes an angle α with the z axis at time t. That is

$$v_z = (v_e^2 - v_x^2)^{1/2} \tag{6c}$$

$$\alpha = \text{arctg}\ \frac{v_x}{v_z} = \frac{dx}{dz}$$

$$= \frac{2\pi A_e}{\lambda_e} \cos \frac{2\pi}{\lambda_e} z(t). \tag{6d}$$

The maximum of α is

$$\alpha_M \equiv 2\pi A_e/\lambda_e. \tag{7}$$

When $2\pi A_e \ll \lambda_e$, one can write $|v_x| \lesssim (2\pi A_e/\lambda_e)v_e$, so that

$$v_z \approx v_e + 0\,[(2\pi A_e/\lambda_e)^2], \tag{8}$$

and $v_z = v_e$ up to second order in α_M.

The electrons interact with an electromagnetic plane wave of wavelength λ. The plane wave travels in vacuum (except for the electrons with which it interacts); thus its angular frequency is $\omega = 2\pi c/\lambda$. The momentum of the plane wave is parallel to the (x,z) plane and makes an angle ψ with the z axis (see Fig. 3). The electric field associated with the wave points along an axis that is obtained by rotating the x axis by ψ around $\mathbf{z} \times \mathbf{x}$. The value of the electric field at point x, y at time t is (independent of y)

$$E = E_0 \cos\left\{\omega t - \frac{2\pi}{\lambda}\,[z(t)\cos\psi + x(t)\sin\psi] + \phi_0\right\}. \tag{9}$$

The electric and magnetic force exerted by the electromagnetic wave on the electron are $\mathbf{F}_E$ and $\mathbf{F}_B$ respectively. Their components are

$$F_{Ex} = Ee\cos\psi, \qquad F_{Bx} = \frac{v_e}{c} Ee\cos\alpha,$$

$$F_{Ez} = -Ee\sin\psi, \qquad F_{Bz} = \frac{v_e}{c} Ee\sin\alpha,$$

$$F_{Ey} = 0, \qquad F_{By} = 0$$

The total electromagnetic force exerted on the electron by the wave is

$$\mathbf{F} = \mathbf{F}_E + \mathbf{F}_B.$$

The longitudinal component (i.e., the component parallel to the instantaneous electron velocity) is

$$F_\parallel = \mathbf{F}\,\frac{\mathbf{v}_e}{|\mathbf{v}_e|} =$$

$$Ee\{[\cos\psi - \frac{v_e}{c}\cos\alpha]\sin\alpha + [-\sin\psi + \frac{v_e}{c}\sin\alpha]\cos\alpha\}, \tag{10a}$$

while its tranvserse component along the direction $\mathbf{y} \times \mathbf{v}_e$ is

$$F_\perp = \mathbf{F} - F_\parallel \frac{\mathbf{v}_e}{|\mathbf{v}_e|} = Ee\Big\{[\cos\psi - \frac{v_e}{c}\cos\alpha]\cos\alpha - [-\sin\psi + \frac{v_e}{c}\sin\alpha]\sin\alpha\Big\}. \tag{10b}$$

Substitution of Eqs. (6) and (9) in Eqs. (10) gives $F_\parallel$ and $F_\perp$ as a function of time. Fortunately, for our purposes it is not necessary to deal with the full complexity of these equations. First, the velocity changes in the energy modulator turn out to be negligible, so that we can consider v_e a constant, $v_e \approx c$. Furthermore, we will consider cases when $\alpha \ll 1$ and $\psi \ll 1$, which allows us to approximate the trigonometric functions by their power series expansion in α and ψ (except when in the argument of another trigonometric function). In this manner, we may write to a sufficient approximation

$$F_\parallel = Ee\ \alpha/2\ \left[\alpha^2\frac{v_e}{c} - \psi^2 + 2\ \left(1 - \frac{v_e}{c}\right)\right] + (1 - \alpha^2/2)\ \left(\alpha\ \frac{v_e}{c} - \psi\right)\Big\},$$

$$F_\perp = Ee\ \Big\{(1 - \alpha^2/2)\tfrac{1}{2}\Big[\alpha^2\frac{v_e}{c} - \psi^2 + 2\ \left(1 - \frac{v_e}{c}\right)\Big] - \alpha\left(\alpha\ \frac{v_e}{c} - \psi\right)\Big\}.$$

Since $F_\parallel$ is proportional to the first power of the small quantities α and ψ, while $F_\perp$ is at least second order in them, we neglect $F_\perp$ in the following. In $F_\parallel$ we keep only terms proportional to the first power in α and ψ then substitute for α and E:

$$F_\parallel \approx E_0 e\ \frac{v_e}{c}\ \frac{2\pi A_e}{\lambda_e}\ \frac{1}{2}$$

$$\Big\{\Big[\cos\left(\frac{2\pi}{\lambda_e} z - \phi\right)\Big]\ \cos\left(\frac{2\pi}{\lambda} x\sin\psi\right)$$

$$+ \Big[\cos\left(\frac{2\pi}{\lambda_e} z + \phi\right)\Big]\ \cos\left(\frac{2\pi}{\lambda} x\sin\psi\right)$$

$$- \Big[\sin\left(\frac{2\pi}{\lambda_e} z - \phi\right)\Big]\ \sin\left(\frac{2\pi}{\lambda} x\sin\psi\right)$$

$$+ \Big[\sin\left(\frac{2\pi}{\lambda_e} z + \phi\right)\Big]\ \sin\left(\frac{2\pi}{\lambda} x\sin\psi\right)$$

$$-Ee\psi \left\{ (\cos\phi)\cos\left(\frac{2\pi}{\lambda}\, x\sin\psi\right) + (\sin\phi)\sin\left(\frac{2\pi}{\lambda}\, x\sin\psi\right)\right\}, \quad (11a)$$

where

$$\phi \equiv \omega t - \frac{2\pi}{\lambda}\, z\cos\psi + \phi_0. \quad (11b)$$

When

$$a \equiv \frac{2\pi A_e}{\lambda}\sin\psi \ll 1, \quad (12a)$$

we can write, with Eqs. (6),

$$\cos\left[\frac{2\pi}{\lambda}\, x\sin\psi\right] \approx 1 - \alpha^2/2\sin^2\left(\frac{2\pi}{\lambda_e}\, z\right), \quad (12b)$$

$$\sin\left[\frac{2\pi}{\lambda}\, x\sin\psi\right] \approx a\sin\frac{2\pi}{\lambda_e}\, z. \quad (12c)$$

Provided that a is small enough, the first of these expressions will not change sign, while the second may. Provided furthermore that

$$\frac{1}{\lambda_e} = \frac{1}{\lambda}\left(\frac{c}{\tilde{v}_z} - \cos\psi\right), \quad (13)$$

from Eq. (6b) $t = (z - z_0)/\tilde{v}_z + t_0$, and

$$\cos\left[\frac{2\pi}{\lambda_e}\, z - \phi\right] = \cos\phi_0 \quad (14a)$$

$$\phi_0 \equiv -\omega\left(t_0 - \frac{z_0}{\tilde{v}_z}\right) - \phi_0 \approx \frac{2\pi}{\lambda}(z_0 - ct_0) - \phi_0. \quad (14b)$$

Clearly, if Eq. (13) holds, $\cos[(2\pi/\lambda_e)z - \phi]$ does not depend on z. When Eqs. (12) and (13) are satisfied, the energy gained by an electron passing through the energy modulator will be

$$\delta E_e = \int_{z_0}^{z_0+L} dz\, F_\parallel(z) = E_0 e\, \frac{2\pi A_e}{\lambda_e}\, \frac{v_e}{c}\, \tfrac{1}{2}(\cos\phi_0)\int_{z_0}^{z_0+L} dz\,\left(1 - \alpha^2/2\sin^2\frac{2\pi}{\lambda}\, z\right) + \text{small terms}. \quad (15)$$

The main contribution to δE_e is due to the first term in the first curly bracket in Eq. (11a). The rest of the terms oscillate as a function of z, their integral over a large enough L will be relatively small; we neglect these "small terms".

With $v_e \approx c$ and Eqs. (7) and (12),

$$\delta E_e \approx eE_0\, \alpha_M/2\ (\cos\phi_0)\, L\,(1 - s) \quad (16a)$$

$$s \equiv \tfrac{1}{2}(\alpha_M\sin\psi)^2\,\frac{1}{L} \times \int_{z_0}^{z_0+L} dz\,\sin^2\frac{2\pi}{\lambda}\, z \underset{L\to\infty}{\longrightarrow} \tfrac{1}{4}(\alpha_M\sin\psi)^2. \quad (16b)$$

Clearly, if conditions (12) and (13) are satisfied, an electron passing through the energy modulator will gain an amount of energy that is approximately proportional to L. The energy gain may be positive (if $-\pi/2 < \phi_0 < \pi/2$) or negative (if $\pi/2 < \phi_0 < 3\pi/2$) or zero (if $\phi_0 = \pm\pi/2$). If for some z_0 the cos $\phi_0 = 1$, then for $z_0 + \lambda/2$ one has cos $\phi_0 = -1$. Electrons located in one $\lambda/2$ long section of the beam will increase their energy as a result of passing through the energy modulator, while electrons in the next region of the same length will decrease their energy during passage through the device. If the wavelength λ lies in the optical region, then energy gain and loss can thus be induced within an optical wavelength.[10]

In the energy modulator as just described, all electrons move along a sinusoidal path. One could instead let the electrons travel along helical paths; the formulae valid for that case are similar to the ones just given.

Beam Buncher. The purpose of this device is to transform the energy modulation into beam-density variation. The path followed by an electron is deliberately arranged to be a sensitive function of the electron energy E_e. The shape of the paths can be chosen to suit the range of parameters with which one has to work. Here we shall discuss one of the simplest possibilities.

The electron trajectory in the beam buncher is shown by a solid line in Fig. 4. (The arcs indicated by dash-dot lines and the angle φ_1 will be discussed later.) The beam buncher has total length D and is

divided into three sections. The first and third are $D/4$ long, while the second has length $D/2$. The electron enters at $z = 0$ with velocity parallel to the z axis. Its trajectory is a sequence of three smoothly joined circular arcs. The length of the trajectory in the first, second and third sections has lengths respectively $S/4$, $S/2$ and $S/4$. We have from Fig. 4,

$$\tfrac{1}{4}S = R\varphi \quad \text{and} \quad \tfrac{1}{4}D = R\sin\varphi,$$

so that

$$S = D + \tfrac{2}{3}\, R\varphi^3(1 - \varphi^2/_{20}\,\varphi^2) + 0\,(R\varphi^7). \quad (17)$$

Expanding $\varphi = \arcsin(D/4R)$ in powers of $u = D/R$, one obtains

$$S = D + {}^1/_{96}\, Du^2\,[1 - 2.813 \cdot 10^{-2}\, u^2 + 1.041 \cdot 10^{-3}\, u^4 + 0(u^6)]. \quad (18)$$

The radius R is proportional to E_e. When E_e changes by an amount $\delta E_e \ll E_e$, *then* R changes by $\delta R \ll R$, and S changes by an amount

$$\delta S = \frac{1}{96}\, Du^2 \left\{ -2\frac{\delta R}{R} + 3\left(\frac{\delta R}{R}\right)^2 + 0\left[\left(\frac{\delta R}{R}\right)^3\right]\right\} f(u)$$

$$f(u) = [1 - 5.626 \cdot 10^{-2}\, u^2 + 0(u^4)] \quad (19)$$

Thus, if two electrons enter the beam buncher at the same time, but one has energy E_e, while the other has $E_e + \delta E_e$, the former electron will leave the device first, and at that moment will be be ahead of the latter electron by δS.

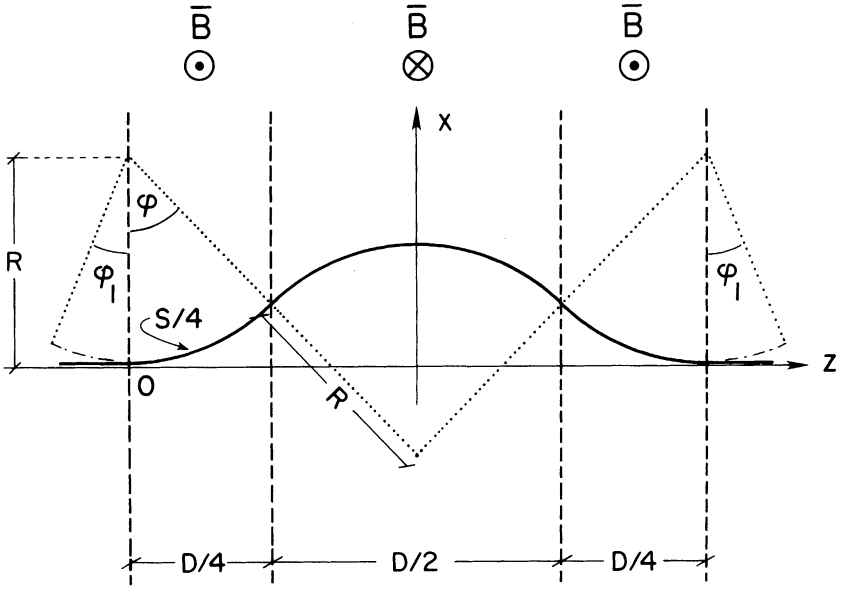

FIGURE 4. The beam buncher has total length D. It consists of three sections: the first and third have length $D/4$, the second $D/2$ long. The magnetic field **B** is uniform in each section, perpendicular to the plane of the drawing, and its orientation is shown for all three sections. The field intensity is the same in all sections. An electron travels along the solid curve. It enters the beam buncher at $z = 0$. There its velocity is parallel to the z axis. Due to the presence of the magnetic fields, the electron trajectory consists of three smoothly joined circular arcs of radius R. The length of the first and third arc is $S/4$, that of the second is $S/2$.

When the magnetic field in the energy modulator is uniform, one may prefer to have the electrons enter and leave the buncher not parallel to the z axis, but at an angle φ_1, along the arcs drawn with dash-dot lines.

The energy change induced in the energy modulator is the same for electrons at positions z and $z + n\lambda$ (where n is any integer); the energy modulation will be periodic in z with a period λ; therefore the beam-density modulation produced is also periodic by λ in z.

It is important to notice that this periodicity need not be simple harmonic. Instead, it may contain a significant admixture of much shorter wavelength Fourier components $\lambda_m \ll \lambda$. The amplitude of these components depends on the parameters of the beam buncher. When λ is in the optical range, λ_m may be in the x-ray region.

We now study the density function produced by that particular beam buncher for which Eq. (19) holds. Since the density is periodic, it suffices to investigate those electrons which at time t_0 (before traversing the buncher) are located in the interval $-\frac{1}{2}\lambda < z \leq \frac{1}{2}\lambda$. Without loss of generality one may choose the reference point in time so that

$$\frac{2\pi}{\lambda} ct_0 + \phi_0 = -\frac{3}{2}\pi, \tag{20}$$

which implies

$$\cos \phi_0 = \sin 2\pi \frac{z_0}{\lambda} . \tag{21}$$

Since in the buncher $r \sim E_e$, one has $\delta R/R = \delta E_e/E_e$. To simplify discussion, consider only the important case when $\psi = 0$. Then Eqs. (16) and (19) give

$$\delta S = -\frac{D}{48} u^2 f(u) \frac{\delta E_e}{E_e} \left\{ \sin \frac{2\pi z_0}{\lambda} + 0 \left[\left(\frac{\delta E_e}{E_e} \right) \sin^2 \frac{2\pi z_0}{\lambda} \right] \right\} . \tag{22}$$

Typically, $\delta E_e/E_e \approx 10^{-5}$ for a high-energy storage ring. Therefore, for most purposes the second term in the curly bracket can be neglected. In this approximation, δS goes to zero as z_0 does: an electron located at $z_0 = 0$ when $t = t_0$ will travel a distance S while traversing the buncher to a point which we denote by $z_f(0)$. Electrons with slightly larger z_0 values will have a negative δS: after traversing the buncher, they will be displaced towards $z_f(0)$ and end up at point $z_f(z_0)$.

Let us concentrate our attention on electrons with sufficiently small z_0, so that $\sin 2\pi z_0/\lambda$ can be approximated by a power series. (The other electrons will give a more slowly varying "background" density distribution, which is of less interest to us at the moment.) For these

$$\delta S \approx -\frac{D}{48} u^2 f(u) \frac{\delta E_e}{E_e} \frac{2\pi z_0}{\lambda} \left\{ 1 - \frac{1}{6} \left(\frac{2\pi z_0}{\lambda} \right)^2 \right\}. \tag{23}$$

If one chooses

$$\frac{D}{48} u^2 f(u) \frac{\delta E_e}{E_e} \frac{2\pi}{\lambda} = 1, \tag{24}$$

then in the first approximation (when the second term in the curly bracket can be neglected) Eq. (23) gives $\delta S = -z_0$ so that as a result of traversing the buncher, all electrons will end up at the same point together with that electron which at $t = t_0$ was at $z_0 = 0$, i.e., at point $z_f(0)$. In this approximation, $z_f(z_0) = z_f(0)$ for all z_0. The density will be infinite at the "catastrophic point" $z_f(0)$. In the second approximation the density is finite, but high at $z_f(0)$ (see Fig. 5). The result is a density distribution ρ which falls off as $z_f^{-2/3}$ near the points $z_f(0) + n\lambda$, where n is any integer. This $\rho(z_f)$ is of the type illustrated in Fig. 1 by the solid line.

Fourier Transform of ρ. To calculate the Fourier transform, $F(\omega)$, of $\rho(z_f)$, one must know ρ for all z_f, but to calculate $F(\omega)$ for $\omega \gg 2\pi/\lambda$, it suffices to know the behavior of ρ near $z_f(0)$. In our case, for z_f near $z_f(0)$ one has $\rho \sim z_f^{-2/3}$. Therefore,

$$F(\omega) \sim \omega^{-1/3} \tag{25}$$

for $\omega \gg 2\pi/\lambda$. Evidently, ρ is rich in high Fourier components: ω can be increased by a factor of a thousand before $F(\omega)$ decreases by one order of magnitude.

The validity of our approximation is limited by the second term in the curly bracket in Eq. (22). In practice, a more severe limitation is presented by the accuracy with which the guiding fields can be maintained in the ring and by the finite momentum and energy spread of the circulating beam.

Bootstrapping the modulation frequency. Once the beam modulation is sufficiently high to produce soft

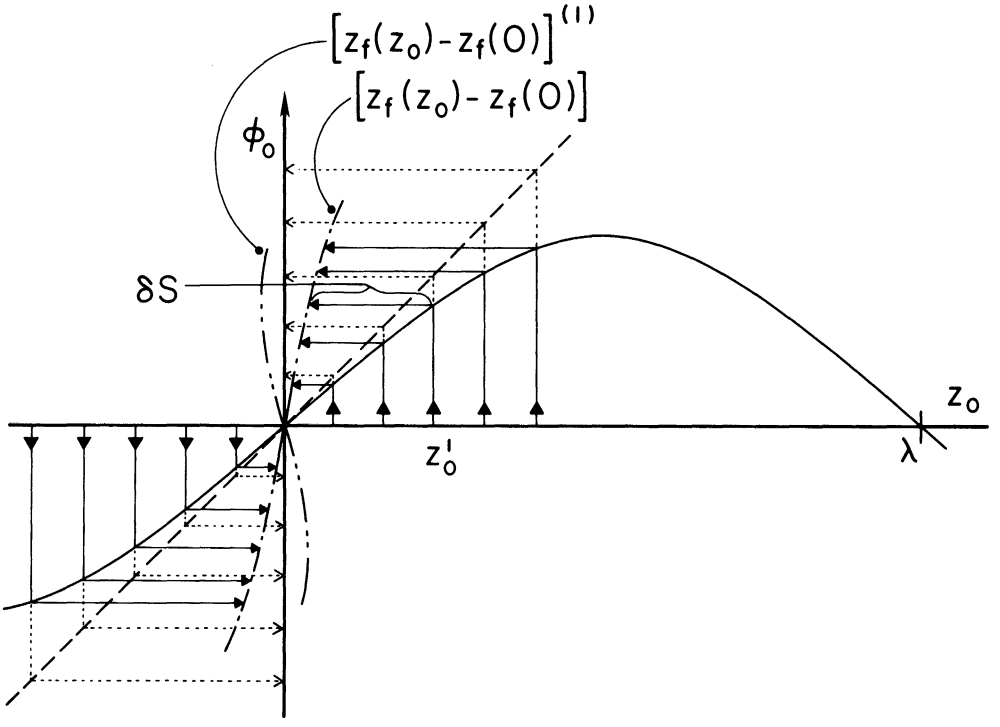

FIGURE 5. The quantity $[z_f(z_0)-z_f(0)]$ is shown as a function of z_0. Is is assumed that t_0 is chosen so that $\cos\phi_0 = \cos 2\pi z_0/\lambda$, and the solid curve shows ϕ_0 as a function of z_0. In part of the figure it is also assumed that Eq. (24) holds, so that $\delta S = -\cos\phi_0$. The δS is indicated for one particular z_0 value: z_0^1. To find the quantity $[z_f(z_0)-z_f(0)]$ for any z_0, draw lines as shown by the arrows: first a vertical line from z_0 to the solid curve, then from there a horizontal line to the dash-dot curve. The distance between the dash-dot curve and the vertical axis is $[z_f(z_0)-z_f(0)]$. For small z_0/λ, the approximation to Eq. (23) is shown by the dotted horizontal arrows: $[z_f(z_0)-z_f(0)]=0$.

When the left hand side of Eq. (24) > 1, the dash-dot curve is to be replaced by a curve like the dash-double-dot line.

x-rays in large enough quantities for pumping a soft x-ray laser[11] (e.g., Li II or Li III laser), one may use the collimated coherent radiation generated by this laser as the electromagnetic wave in a second energy modulator. The procedure described earlier can now be repeated with this wave, so that in principle one can induce a fundamental harmonic in the electron density which lies in the soft x-ray region as well as higher harmonics of even shorter wavelength. These harmonics will then enhance the intensity of x-rays emitted by the beam in this shorter wavelength region. Those x-rays may in turn be used to pump a shorter wavelength x-ray laser, etc.

Practical realization of this sequence of "bootstrapping" steps will be more difficult as higher modulation frequencies are reached. Partly because to pump a shorter wavelength x-ray laser one needs higher instantaneous pumping photon brightness, partly because the tolerances on guiding fields in the energy modulator, beam buncher, etc., are then smaller, and partly, because higher electron density is required if n is to be the same for smaller λ_m.

Finite Momentum and Energy Spread. To simplify our discussion, we assume that the vertical momentum spread $\Delta p_y \approx p\Delta y'$ is negligible (otherwise Δp_y can be treated as Δp_x will be).

The horizontal momentum spread Δp_x can be neglected, provided that it is smaller than some critical Δp_0

$$\Delta p_x < \Delta p_0 \equiv p\Delta x_0'. \tag{26}$$

(the value of $\Delta x_0'$ will be evaluated later). In such a case, the discussion of the preceding sections is valid. When Δp_x violates condition (26), our aim is to change the electron phase-space distribution so the inequality (26) should hold.

Changes in the electron phase-space volume are illustrated in Figs. 6a–f. In these figures three-dimensional projections of the (six-dimensional) electron phase-space volume are shown. For ease of illustration, a step-function-like (unrealistic) phase-space distribution is assumed. With this unrealistic distribution the (x,x') phase space ellipse is idealized as a "phase-space quadrangle", as can be observed by looking at the projection of the distributions onto the (x,x') plane.

Spreading the Beam. It is assumed that originally (at point z_a along the orbit) the total horizontal angular spread $\Delta x_a'$ violates condition (26). The point z_a is so chosen that here the horizontal phase-space quadrangle is "upright", i.e., its neighboring sides are orthogonal to each other (Fig. 6a).

To reduce $\Delta x'$, the beam is first allowed to spread along the x axis. This increases Δx, but leaves $\Delta x_a'$ as well as the total phase-space volume unchanged. By the time the electrons reach z_b, the phase-space volume has assumed the shape shown in Fig. 6b. Next the electrons are focused so that when they arrive at point z_c, the phase-space quadrangle is again "upright", but now $\Delta x' = \Delta x_c'$ satisfies inequality (26) (see Fig. 6c).

Since the focal length of a magnetic lens depends on the electron energy E_e, at z_c some correlation exists between E_e and x. This correlation causes an additional momentum spread δp_x along the x axis. Denoting by E_{e0} the nominal electron energy, one can show that (in the thin-lens approximation) $\delta p_x < 2p\,|\,\Delta x_a'\,|\,\Delta E_e/E_e$. We neglect δp_x in what follows.

Energy Separator. Its purpose is to induce a strong correlation between E_e and x. In principle it can be a simple device. For example:

Let an electron travel a distance l in a homogeneous magnetic field. As a result, the electron will change its direction by $\Theta \approx l/R$. For an electron whose energy is the nominal energy E_{e0}, one has $\Theta = \Theta(E_{e0})$, while for electrons with some other energy $E_e = E_{e0} + \frac{1}{2}\,\Delta E_e$, the angle is

$$\Theta(E_e) = \Theta(E_{e0})\,[1 + \tfrac{1}{2}\Delta E_e/E_{e0}],$$

since $\Theta \sim R^{-1} \sim E_e^{-1}$. If the electrons are now allowed to travel a distance H in a force-free vacuum to point z_c, the distance Δx between these two electrons perpendicular to the momentum of the ideal electron will be

$$\tfrac{1}{2}\Delta x_d = H \sin\frac{\Delta\theta}{2} \approx \tfrac{1}{2}H\theta(E_{e0})\,\Delta E_e/E_{e0}. \tag{28}$$

Subsequently the electrons are focused to form an essentially parallel beam. At any point x, the beam will contain electrons with energy lying within an interval of total width

$$\Delta_I E_e \approx \Delta x_c/\Delta x_d. \tag{29}$$

The resulting phase-space volume is illustrated in Fig. 6d. At this stage Δp_x is negligible and $\Delta_I E_e \ll \Delta E_e$. Next the electrons traverse the energy modulator, where their energy is altered by δE_e, as given in Eq. (16). This alteration will not be washed out by the background energy spread, provided that

$$\tfrac{1}{2}E_0 e\alpha_M L \gtrsim \tfrac{1}{2}\,\Delta_I E_e. \tag{30}$$

Note that if the energy separator is omitted, i.e., if the step illustrated in Fig. 6d is absent, then it would still be possible to induce in the beam the desired density variation, but only if one satisfied the condition

$$\tfrac{1}{2}E_0 e\alpha_M L \gtrsim \tfrac{1}{2}\,\Delta E_e. \tag{30a}$$

For given $\alpha_M L$, the energy separator thus allows a reduction in E_0 by a factor $\Delta E_e/\Delta_I E_e$. Since the power of an electromagnetic wave is proportional to E_0^2, this will lead to a large reduction of the (e.g., laser) power requirements when $\Delta_I E_e/\Delta E_e \ll 1$.

The α_M decreases with E_e if the magnetic field in the energy modulator is fixed. Therefore, δE_e will be smaller for higher-energy electrons. One may have to compensate for this. A magnetic field will accomplish such a compensation if its gradient along x has the appropriate (positive) value (see Fig. 6d).

In an alternative approach, the magnetic field in the energy modulator may be uniform, and compensation is achieved by making the electrons enter the beam buncher at an angle φ_1 (dash-dot line in Fig. 4) instead of entering along the axis (solid line in Fig. 4). In this manner, choosing $\varphi_1 < 0$, one can insure that for electrons with larger x (and thus E_e) the pathlength in the beam buncher is longer by an

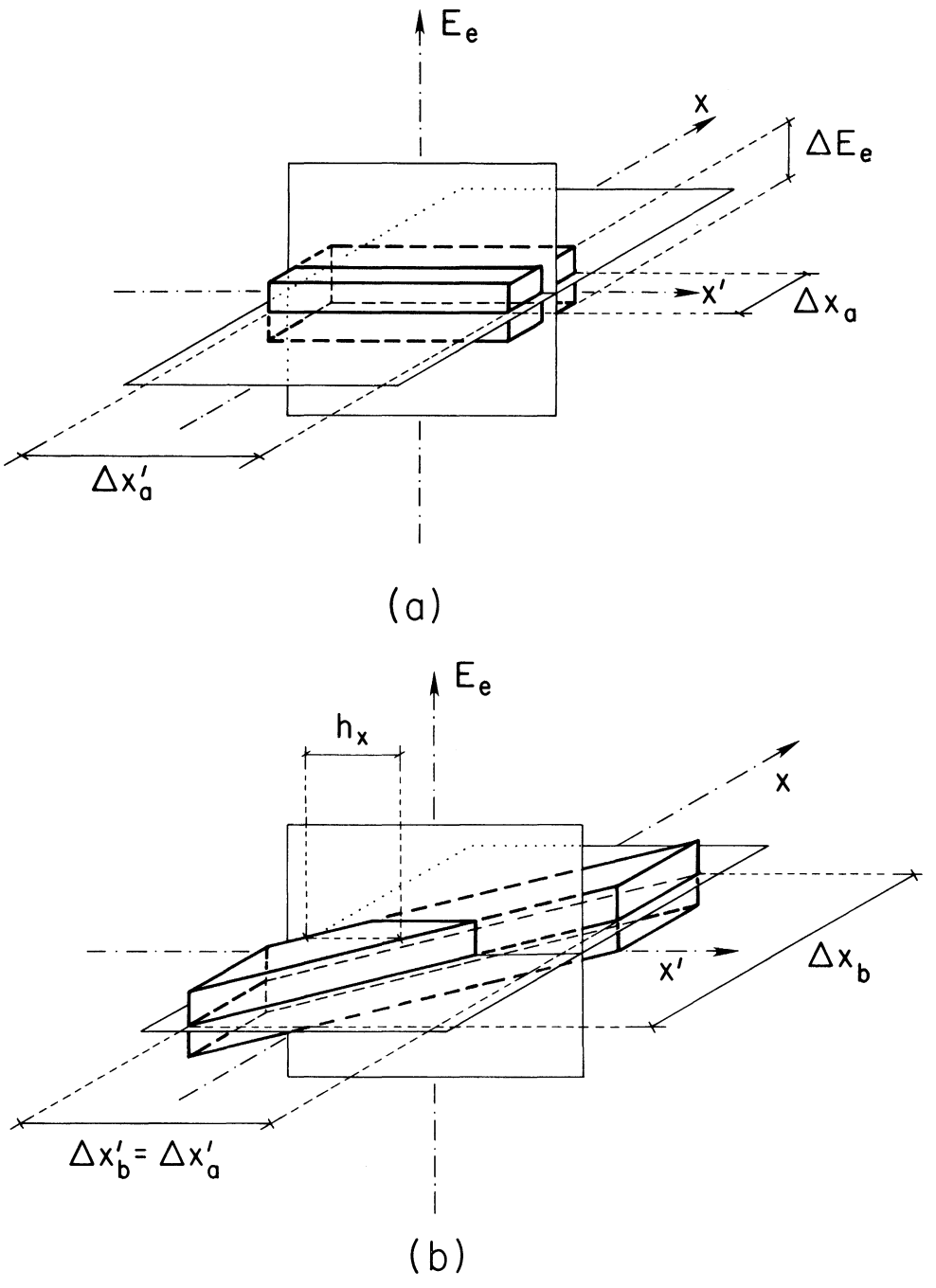

FIGURE 6. Projections of the (six dimensional) electron phase space are shown. Step-function-like (unrealistic) distributions are assumed to simplify illustration.

a. Three-dimensional projection of the electron phase space at some point z_a along the orbit. The full beam width along x is Δx_a, the total angular spread in the horizontal plane is $\Delta x'_a$ and the full spread in the circulating energy E_e, is ΔE_e. The $\Delta x'_a$ is assumed to be larger than the critical $\Delta x'_0$.

b. By the time the electrons reach point z_b along their trajectory, the beam width along x has increased to Δx_b. Now for any value of x the total angular spread is $\leq h_x < \Delta x_0$, but the total angular spread in the horizontal plane is still $\Delta x'_b = \Delta x'_a$.

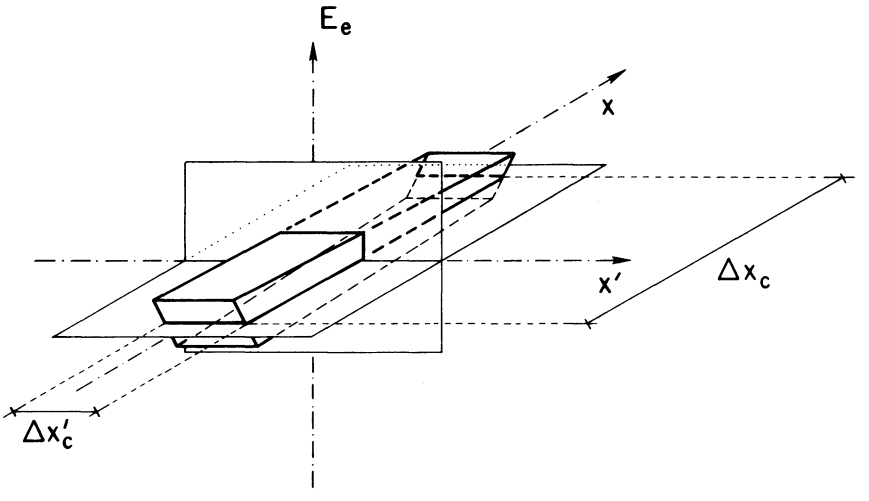

(c)

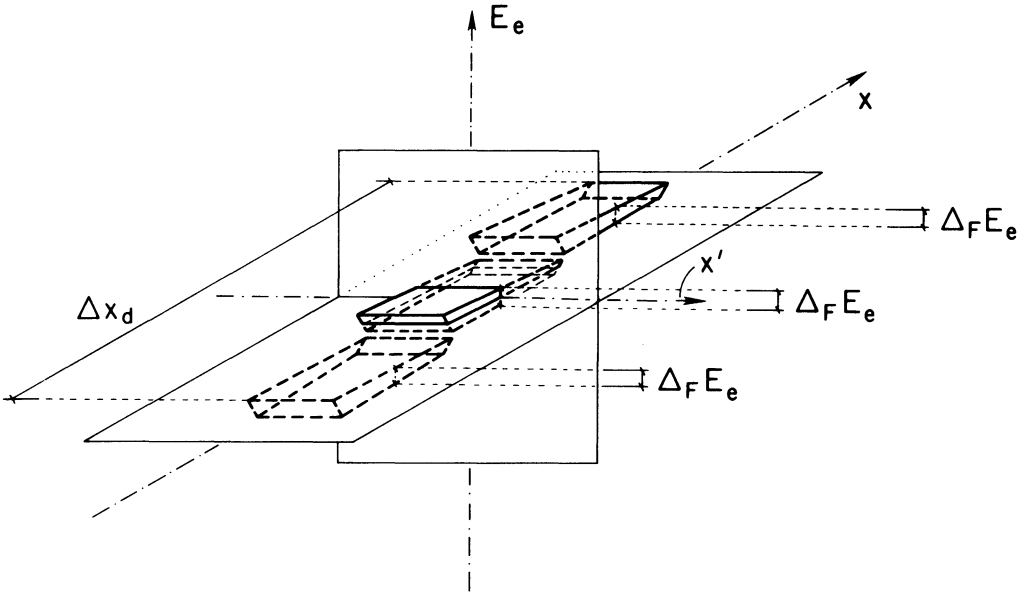

(d)

c. At point z_c the angular spread is reduced from $\Delta x'_b$ to $\Delta x'_c = h_x$, while $\Delta x_c = \Delta x_b$ is unchanged. The far and near ends of the illustrated phase-space projection are vertical quadrangles (parallel to the $[x', E_e]$ plane). Neighboring sides of these quadrangles are not perpendicular, because electrons with higher than average circulating energy are focused less. After this point, the electrons enter the energy separator.

d. The energy separator induces a correlation between the circulating electron energy E_e and x. The total width of the beam is further increased to $\Delta x_d > \Delta x_c$. The figure shows the phase space at point z_c, just after the electrons leave the energy separator. To make illustration easier, the phase-space volume is assumed to consist of three disconnected pieces. Dashed line means that it is below the $[x', x]$ plane, or behind the $[x', E_e]$ plane, or both. (In reality the phase-space volume is continuous.) Each piece has an energy spread $\Delta_F E_e < \Delta E_e$. The result is that at any chosen value of x the energy spread is less than in Fig. a, b, or c. The ratio $\Delta E_e / \Delta_F E_e$ can be large, if $\Delta x_d / \Delta x_c$ is. After this stage the electrons enter the energy modulator.

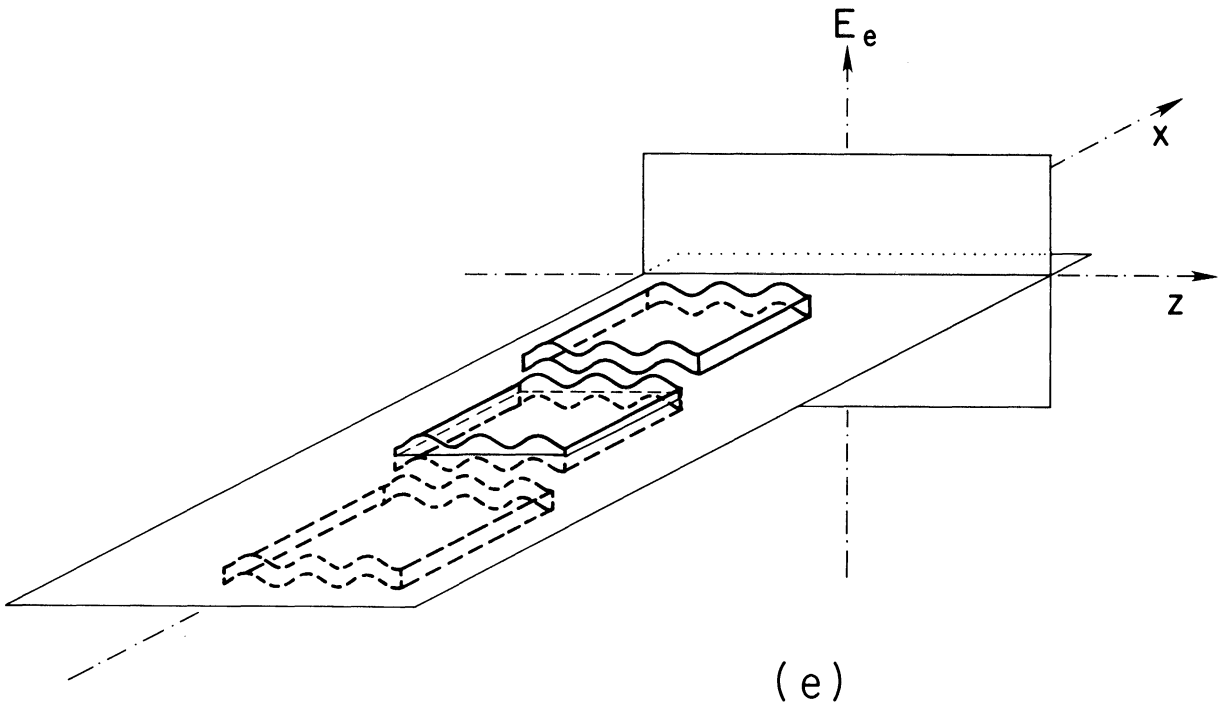

(e)

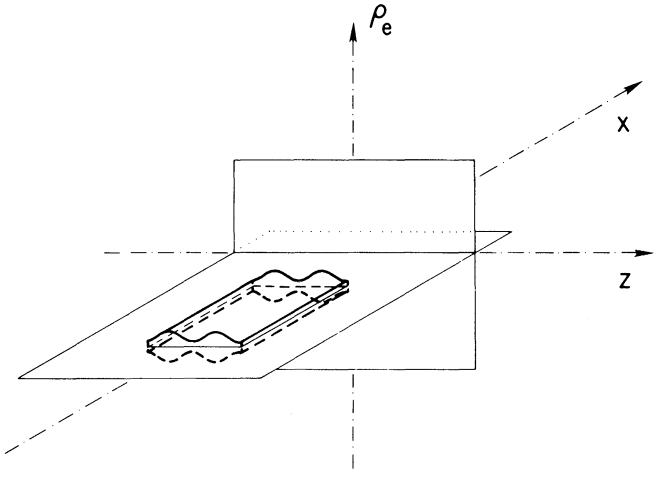

(f)

e. The energy modulator changes the energy of the electrons. The energy change is a function of the z coordinate. (Note the change of axis.)

f. Electrons enter the beam buncher. Those with higher energy will fall behind, while those with lower energy get ahead of electrons of average energy. The result is a beam-density modulation of optical and suboptical dimensions.

amount

$$\delta\phi_1 = \phi_1 R \frac{E_e - E_{e0}}{E_{e0}} = (\text{const})\, x \qquad (31)$$

The phase of the electromagnetic wave in the energy modulator contains a term $2\pi\sin\psi$, and since by assumption $E_e \sim x$ (see Fig. 6d), all electrons with the same ϕ_0 will have the same z coordinate (modulo λ) after the buncher, if the constant on the right-hand side of Eq. (31) satisfies

$$-2\pi \sin\psi = \text{const.}$$

Refocusing. For certain applications, one more step is needed: the beam has to be refocused and its cross section reduced in order to achieve high electron density while the beam radiates the photons of interest in the region of space of interest (e.g., synchrotron-radiation photons while passing in front of the exit port; coherent photons between the mirrors of a free-electron laser, etc.). The Δp_x can be large here, subject only to the condition that high electron density and its modulation should persist throughout the region of interest.

To insure that refocusing will not wash out a density modulation with wavelength λ_m, all electrons have to arrive at the focal plane with a time accuracy of $\pm\lambda_m/8c$. In principle this can always be done; an electron located at point (x_i,z) before refocusing will travel a distance $l \approx f + \frac{1}{2} x_i^2/f$ to the focal point, if $f \gg x$ is the focal length. All electrons which have the same z coordinate before refocusing, and for which $|x_i| \leq \frac{1}{2}\Delta x$ will reach the focus with the required time accuracy, provided that

$$f \gtrsim \tfrac{1}{2}(\Delta x)^2/\lambda_m. \qquad (32)$$

In practice, as in the example to be given below, one may prefer to induce in the beam a correlation between E_e and y (instead of x). To illustrate this case, one should replace x by y in Figs. 6d and 6e. Proper timing is then insured by the inequality obtained from (32) by replacing in it Δx by Δy. Since usually $\Delta y \ll \Delta x$, for this case smaller f will suffice.

Determination of $\Delta x_0'$

To lowest order, conditions on $\Delta x'_0$ can be obtained as follows. Electrons entering the energy modulator at an angle $\frac{1}{2}\Delta x'_0$ will gradually get out of phase with the electromagnetic wave unless

$$L\,[\cos(\psi \pm \tfrac{1}{2}\,\Delta x_0')]^{-1} - L\,(\cos\psi)^{-1} \lesssim \lambda/4. \qquad (33a)$$

Furthermore, the electrons will deviate by Lx'_0 from the design orbit at the far end of the energy modulator, which will wash out the correlation between E_e and x, unless

$$L\,\tfrac{1}{2}\,\Delta x'_0 \lesssim \tfrac{1}{4}\,\Delta x_c. \qquad (33b)$$

Similar (lowest-order) considerations for the beam buncher and for the process of refocusing (if needed) lead to the additional conditions

$$\Delta x'_0 \lesssim [2\lambda\,(S+f)^{-1}]^{1/2},$$

$$\Delta x_0' \lesssim \tfrac{1}{2}\,\frac{\Delta E_e}{\Delta_F E_e}\,\frac{\Delta x_c}{S}\,,\ \tfrac{1}{2} f^{-1}\Delta x_f, \qquad (33c)$$

where Δx_f is the total horizontal beam diameter to be achieved after refocusing.

Compensation: Defocusing, beam debunching, energy demodulation. The length of an electron trajectory around the storage ring may vary by more than λ from one turn around the ring to the next, or, at any rate, after a few turns around the ring. An electron which gained energy during one traversal through the energy modulator may either gain or lose energy during the next traversal, or any one of the following traversals. Therefore the average energy gained by an electron will increase with time as $t^{1/2}$. To avoid blowing up the beam, the average energy gained by an electron during one traversal of the energy modulator must not exceed the average energy radiated away by the electron during one trip around the ring. This condition limits δE_e.

That limitation can be circumvented as follows. After the bunched beam emits the desired photons, we immediately undo what we did to the beam to bunch it. As an illustration, imagine that one takes a motion picture of the electrons as they change their energies while moving through the beam buncher, and eventually the emergence of electron bunches after traversing the beam buncher. Running this motion picture backwards, it would show the disappearance of bunches as the electrons move backwards through the beam buncher, and finally, all

TABLE I

The first part of the table gives the beam characteristics of the storage ring. The values are similar to those calculated for SPEAR in single-beam mode operation, when the horizontal-vertical coupling is $\kappa = 0.1$, and when the magnets are tuned for this operating mode. The circulating electron energy is E_e, and $\Delta E_e/E_e$ is the full width of the gaussian energy spread, ϵ_x and ϵ_y the horizontal and vertical emittance, $2\sigma_0 = \Delta z$ the full gaussian bunch length.

The second part of the table refers to the energy separator, i.e., the device which takes the beam phase space from a configuration illustrated in Fig. 6c, to one similar to what is shown in Fig. 6d. Before entering the energy separator, the beam has horizontal (r.m.s.) diameter Δx_c and total horizontal (r.m.s.) angular spread $\Delta x_c'$. After leaving the energy separator, the corresponding values are Δx_d and x_d'. The Δy_c, $\Delta y_c'$, Δy_d and $\Delta y_d'$ are defined similarly. Note that whereas in Fig. 6d the energy is correlated with the x coordinate ($\Delta x_d > \Delta x_c$), here we assume that the energy separator correlates E_e with the y coordinate, therefore now $\Delta y_d > \Delta y_c$. The ratio $\Delta y_d/\Delta y_c \approx \Delta E_e/\Delta_F E_e = 25$.

The third part of the table describes the parameters of the energy modulator, i.e., the device in which (see Fig. 3) an electromagnetic wave of wavelength λ and (electric) amplitude E_0 modulates the energy of electrons moving along an approximately sinusoidal path of wavelength λ_e and amplitude A_e. The maximum angle which the electron path makes with the z axis is α_M and the maximum energy transferred to the electrons is δE_M. The electromagnetic wave travels along a line whose direction makes an angle ψ with the z axis. The static magnetic field in the modulator is B^s. Choose the $\psi = 0$ and $B_x^s = 0$. To insure that the energy spread of the electrons will not wash out the effect of the energy modulator, the static field gradients $\partial_y B_y^s$ and $\partial_z B_z^s$ are non-zero. At the center of the modulator the magnetic field has components B_{0y}^s and B_{0z}^s. R is the average radius of curvature of the electron trajectory in the modulator. The beam dimensions in the modulator are as in the energy separator: Δx_d, Δy_d (listed in the first part of the table).

The electromagnetic field is assumed to be produced by a laser, synchronized with the circulating electron bunch. The laser pulse is assumed to fill a cylinder with horizontal and vertical diameters $2\Delta x_d$, $2\Delta y_d$, and $2.5\ \Delta z$ long.

The fourth part refers to the beam buncher. The beam dimensions are approximately as in the energy modulator: Δx_d, Δy_d. The magnetic field is B_b. The radius of curvature for an electron with circulating energy 2.5 GeV is R_b. The length (along z) of the buncher is D. After traversing the buncher, the difference between the z coordinate of an electron which gained $|\delta E_{eM}|$ energy in the modulator, and one which lost $|\delta E_{eM}|$ energy in the modulator, will decrease by δS. To insure effective bunching with $\lambda_m = \lambda$, one needs $\delta S = \lambda/2$ (satisfied here).

Beam Characteristics	E_{e0}	2.5 GeV
	$\frac{1}{2}\Delta E_e/E_e$	$0.5 \cdot 10^{-3}$
	ϵ_x	10^{-1} mm·m rad
	ϵ_y	10^{-3} mm·m rad
	σ_z	1 cm
Energy Separator	$\Delta x_c = \Delta x_d$	4 mm
	$\Delta x_c' = \Delta x_d'$	0.1 m rad
	Δy_c	0.1 mm
	$\Delta y_c' = \Delta y_d'$	10^{-2} m rad
	Δy_d	2.5 mm
	$\Delta_F E_e$	50 keV
Energy Modulator	λ	10^{-4} cm
	E_0	$1.22 \cdot 10^5$ V/cm
	λ_e	12 cm
	A_e	$6.12 \cdot 10^{-3}$ cm
	α_M	$4.08 \cdot 10^{-3}$
	δE_e	50 keV
	ψ	0
	Δz	2 cm

	B^s_{y0}	10.2 kG
	B^s_{z0}	0
	$\partial_y B^s_y$	2.04 kG
	$\partial_z B^s_z$	−2.04 kG/cm
	R	$7.35 \cdot 10^2$ cm
	Δz	5 cm
	Energy in one laser pulse	$6.26 \cdot 10^{-4}$ J
	Instantaneous laser power	$3.76 \cdot 10^6$ W
	Average laser power	800 W
	Average laser power with 200 reflections	8.00 W
Beam Buncher	B_b	21.4 kG
	R_b	$3.51 \cdot 10^2$ cm
	D	$1.94 \cdot 10^2$ cm
	$u^2 = D^2/R^2$	0.308
	ΔS	$5 \cdot 10^{-5}$ cm

electrons regaining their original energy, as a result of their traversing backwards through the energy modulator. Since electromagnetic interactions are time-reversal invariant, and the beam consists of a periodic series of microbunches, the same result can be obtained (except for the first and last microbunch) by running the electrons not backwards, but allowing them to move forward, pass through a "beam debuncher" essentially identical in construction to the beam buncher, and subsequently traverse an "energy demodulator" whose construction is essentially identical to that of the beam buncher.

On the basis of the above argument it is clear that the effects of energy modulation and beam bunching can be compensated in the following manner.

If the beam was refocused after bunching, allow it to continue undisturbed until it unfocuses itself to the same size as it had immediately after the buncher. (If before focusing E increased with y (or x), now E may decrease with y (or x). This difference is inessential, it could be eliminated by one more focusing and subsequent defocusing. If the beam was not refocused after photon emission, it may be led directly into the debuncher. In either case, the beam entering the debuncher should be of the same size as immediately after the buncher. The beam debuncher is a device identical in construction to the beam buncher, except that in it the magnetic-field direction may be reversed. It is followed by the energy demodulator, which is identical in construction to the energy modulator, except that in it too some electric or magnetic fields may be reversed. At any rate, they are so arranged that if an electron gained energy δE_e in the energy modulator, it will lose energy δE_e in the energy demodulator.

Compensation will not be perfect, first, because during emission of the desired photons (at a synchrotron-radiation port, in an undulator or free-electron laser, etc.) electrons undergo random energy changes which will not be compensated. The second, more important reason is that the guiding fields in the storage ring are not perfect. Nevertheless, compensation will be effective because typically it is to take place within a few meters of the beam buncher. Therefore, electron positions have to be maintained with an accuracy about $\lambda/2$ only while the particles are traveling this distance.

Since these devices are essentially identical to those discussed earlier, the conditions imposed by them on $\Delta x'_0$ can be calculated as explained above.

An Example. We assume that a storage ring like SPEAR is used in single-beam mode, with a horizontal-vertical coupling of $\kappa = 0.1$, and that the magnets are tuned for such an operating mode.

The first part of Table III lists the beam characteristics. The values are similar to those calculated for SPEAR in such a mode of operation. The second, third and fourth parts give the parameters relevant to

the energy separator, energy modulator and beam buncher respectively.

It is assumed that the electromagnetic radiation is produced by a laser. In the first approximation there is no net energy transfer from the laser pulse to the electrons, since some electrons will gain energy from it while others give up their energy to enhance the pulse. The same laser pulse can, therefore, be reused. Assuming that we reflect the laser pulse 200 times and thus reuse it 100 times, the average output of the laser can be reduced by a factor of 100. Actually, so large a reduction is not crucial, since the average power output is in any case quite modest. On the other hand, re-passing the same laser pulse in the energy modulator also reduces the necessary laser repetition rate, and that is desirable for simple operation.

If we had not used the energy separator, then the desired beam modulation could still have been achieved, but only with a laser with about 250 times higher power output than the one needed in conjunction with the energy separator.[12]

ACKNOWLEDGEMENTS

While writing this, I greatly benefited from discussions with K.M. Monahan, P.L. Morton, A.P. Sabersky, P.B. Wilson, and H. Winick.

1. Paul L. Csonka, *Particle Accelerators* **8,** 225 (1978); University of Oregon, I.T.S. preprint No. N.T. 059/75 (1975); and Some Coherence Phenomena with Wigglers and Their Applications in *Wiggler Magnets,* Ed. H. Winick and T. Knight, SSRP Report No. 77/05, May, 1977.
2. This was already noted in: Paul L. Csonka, *Particle Accelerators* **7, 9,** (1975) and University of Oregon preprint N.T. 052/74 (1974).
3. For closed circular electron orbits, the reduction in horizontal angular spread would be washed out by the curvature of the orbit. On the other hand, it will be visible when the radiation is produced by a wiggler in which the electron trajectory deviates from the z axis by an angle $\frac{1}{2}\,\Delta\theta_w \lesssim \frac{1}{2}\,\Delta\theta_x$.
4. Paul L. Csonka, *Particle Accelerators* **7,** 255 (1976). For the effect of mutual Coulomb repulsion, see L.A. Rivlin, *JETP Letters* **13,** 257 (1971).
5. A.P. Sabersky and I.H. Munro, in *Picosecond Phenomena,* Ed. C.V. Schenk, E.P. Ippen, and S.L. Shapiro, Springer Verlag Series in Chemical Physics, Vol. 4 (1978).
6. K.M. Monahan, I.H. Munro, and V. Rehn, in preparation.
7. N.A. Vinokurov, A.N. Skrinski, Institute of Nuclear Physics Preprint, USSR Academy of Sciences, June, 1977.
8. A simpler but less energy-efficient version of this method was given in the first of references (1), and in Enhancement of Synchrotron Radiation by Beam Modulation, University of Oregon ITS, preprint No. N.T. 059/75 (1975). The method presently described requires considerably less laser power and allows an increase of radiated output in free electron lasers.
9. H. Motz, *J. Appl. Phys.* **22,** 527 (1951); R.M. Phillips, IRE *Trans. Electron Devices* 231 (1960).
10. When $\psi = 0$, these expressions reduce to the corresponding ones given in Ref. 8.
11. Paul L. Csonka, *Phys. Rev.* **A13,** 405 (1976), and Opportunities to Produce Coherent Soft X-Rays at Stanford, SSRP Report 77/03 (1977).
12. Without the energy separator, the energy spread of the beam would be $\Delta E_e = 1.25$ MeV for all x. In this case $\delta E_e > \frac{1}{2}\,\Delta E_e = 1.25$ MeV would be needed (instead of $\delta E_e \gtrsim \frac{1}{2}\,\Delta_F E_e = 50$ keV). Since δE_e is proportional to E_0, the laser output is proportional to $(\Delta E_e/\Delta_F E_e)^2 = 625$. This is partly compensated by the fact that the electron beam fills a smaller volume when the energy separator is not used. But this decrease is only partly effective because the smallest volume which is filled by the laser pulse is not the beam volume: it is limited from below by diffraction and multiple reflections. A product of all these factors gives about 250.